Density-matrix renormalization-group calculations of excited states of linear polyenes

William Barford,[1,*] Robert J. Bursill,[2] and Mikhail Yu Lavrentiev[1,†]

[1]*Department of Physics and Astronomy, The University of Sheffield, Sheffield, S3 7RH, United Kingdom*
[2]*School of Physics, University of New South Wales, Sydney, NSW 2052, Australia*
(Received 2 January 2001; published 25 April 2001)

We present density-matrix renormalization-group calculations of the Pariser-Parr-Pople-Peierls model of linear polyenes within the adiabatic approximation. We calculate the vertical and relaxed transition energies, and relaxed geometries for various excitations on long chains. The triplet ($1\,^3B_u^+$) and even-parity singlet ($2\,^1A_g^+$) states have a 2-soliton and 4-soliton forms, respectively, both with large relaxation energies. The dipole-allowed ($1\,^1B_u^-$) state forms an exciton-polaron, and has a very small relaxation energy. The relaxed energy of the $2\,^1A_g^+$ state lies below that of the $1\,^1B_u^-$ state. We observe an attraction between the soliton-antisoliton pairs in the $2\,^1A_g^+$ state. The calculated excitation energies agree well with the observed values for polyene oligomers; the agreement with polyacetylene thin films is less good, and we comment on the possible sources of the discrepancies. The photoinduced absorption is interpreted. The spin-spin correlation function shows that the unpaired spins coincide with the geometrical soliton positions. We study the roles of electron-electron interactions and electron-lattice coupling in determining the excitation energies and soliton structures. Electronic interactions play the key role in determining the ground-state dimerization and the excited-state transition energies.

I. INTRODUCTION

The interplay of electron-electron interactions and electron-lattice coupling in linear polyenes results in a wealth of low-lying excitations. Electron-electron interactions induce spin-density-wave correlations in the ground state. The lowest-lying excitations are triplets, which combine to form dipole-forbidden singlet ($^1A_g^+$) excitations. Optical excitations are gapped, lie above the $2\,^1A_g^+$ state, and are essentially ionic in character, that is, there is charge transfer from one site to another. The lowest optically allowed ($1\,^1B_u^-$) state lies below the charge gap,[1] and is thus excitonic in character. For convenience, we show the group theoretic labeling of the states discussed in this paper in Table I.

Electron-phonon interactions result in a dimerized semiconducting ground state. Within the adiabatic approximation, the nonlinear excitations include charged-spinless and neutral-spin-1/2 solitons. Both electronic interactions and electron-lattice coupling lead to a gap in the optical spectrum. In contrast to the interacting limit, however, the $2\,^1A_g^+$ state always lies above the $1\,^1B_u^-$ state in the noninteracting electron-phonon model.

The realization that electronic interactions play a significant role in polyenes came via the experimental observation, by Hudson and Kohler[2] in 1972, that the $2\,^1A_g^+$ state lies below the $1\,^1B_u^-$ state. At the same time, by performing a double-configuration-interaction calculation on the Pariser-Parr-Pople model, Schulten and Karplus[3] demonstrated that the $2\,^1A_g^+$ wave function has a strong triplet-triplet contribution, and has a lower energy than the $1\,^1B_u^-$ state. The triplet-triplet and correlated nature of the $2\,^1A_g^+$ state was further investigated by Tavan and Schulten[4] and other workers.[5] In 1986, Hayden and Mele[6] performed a real-space renormalization-group calculation on the Hubbard-Peierls model of up to 16 sites, and found that the $2\,^1A_g^+$ state was composed of 4 solitons. This 4-soliton nature was also investigated by Su[7] and Wen and Su.[8] Ovchinnikov *et al.* also high lighted the role of electronic interactions, by suggesting that they are largely responsible for the optical gap.[9] In contrast to the strong deviations from the ground-state geometry predicted for the triplet and $2\,^1A_g^+$ state, Grabowski *et al.*[10] predicted that the $1\,^1B_u^-$ state is an exciton-polaron.

The existence of the $2\,^1A_g^+$ state below the $1\,^1B_u^-$ state in polyacetylene thin films was suggested by a number of experiments. Third harmonic generation (THG) and two-photon absorption, in the work of Halvorson and Heeger,[11] indicate that a $^1A_g^+$ state lies below 1.1 eV, while linear absorption, locating the $1\,^1B_u^-$ state, typically rises at 1.8 eV and peaks at 2.0 eV.[12] However, Fann *et al.*[13] performed THG, finding peaks at 0.6 and 0.89 eV, which they interpreted as $^1A_g^+$ and $^1B_u^-$ states virtually coincident at 1.8 eV. The position of the $2\,^1A_g^+$ state is therefore not definitively established. We return to this point in Sec. V when we discuss our own theoretical predictions. For a detailed review of the experimental and theoretical studies of conjugated polymers up to 1992, see Ref. 14.

Electron-electron interactions in π-conjugated systems, such as *trans*-polyacetylene, are conveniently modeled by the one-band Pariser-Parr-Pople model, which includes long-range Coulomb interactions. This semiempirical model has been used extensively to study the excited states of small conjugated molecules with a remarkable degree of success.[15]

TABLE I. The classification of the relevant states.

State	$^1A_g^+$	$^1B_u^-$	$^3B_u^+$
Spatial inversion symmetry	+	−	−
Spin	0	0	1
Particle-hole symmetry	+	−	+
Character	Covalent	Ionic	Covalent

The Peierls model describes the electron-lattice coupling in the adiabatic limit. Thus the Pariser-Parr-Pople-Peierls model is a realistic and accurate model of π-conjugated systems, which captures their essential physics. In an earlier paper[16] we performed accurate calculations on this model using the infinite lattice algorithm of the density-matrix renormalization-group (DMRG) method.[17,18] The Hellmann-Feynman theorem was used to calculate the low-lying excited states and the lattice geometry associated with them. We showed that the $1\,^3B_u^+$ and $2\,^1A_g^+$ states are modeled by 2- and 4-soliton fits, respectively, and that the $1\,^1B_u^-$ state is an exciton-polaron. In this paper we develop that work. In particular, our objectives are the following.

(1) To further demonstrate that the DMRG calculations are reliable by (i) making comparisons to the exact noninteracting limit, and (ii) comparing the infinite-lattice method to the finite-lattice method.

(2) To use a realistic model of polyenes to understand the roles of electron-electron interactions and electron-lattice coupling in determining the dimerization of the ground state and the transition energies of the excited states. In agreement with the earlier work of Horsch[19] and Konig and Stollhoff,[20] we find that electronic interactions play the key role in driving the ground-state dimerization. Electronic interactions are also dominant in determining the solitonic structures and transition energies of the excited states.

(3) To make more detailed comparisons to other experimental probes, in particular photoinduced absorption. The agreement with a wide range of experiments confirms the validity of the model, our calculational method, and our predictions on the soliton structures and their interactions.

(4) To further investigate both the geometry and electronic properties of solitons.

This paper also serves as a correction to Ref. 16. In that paper we use the dimerized ground-state geometry in the Coulomb interactions to calculate the energy of all the states. Thus the Coulomb interactions (unlike the one-electron transfer integrals) were not updated in the Hellmann-Feynman minimization procedure for the relaxed states. We find that using the correct geometry in the Coulomb interactions affects the excitation energies by approximately 0.1 eV. The geometry of the triplet excited state is modified, so that now there is no soliton-antisoliton confinement in the triplet state. However, attractive soliton interactions remain in the $2\,^1A_g^+$ state.

The plan of this paper is as follows. In Sec. II we introduce the Pariser-Parr-Pople-Peierls model. To establish the consequences of the interplay of electron-electron interactions and electron-lattice coupling, we consider these two limits separately in Secs. III and IV. The noninteracting limit also allows us to compare the infinite and finite DMRG algorithms to an exact calculation. In Sec. V we solve the full model, and discuss the vertical and relaxed energies of the key excited states. As well as linear absorption and nonlinear optical spectroscopies, photoinduced absorption is a useful tool in determining the positions of excited states. We discuss the experimental situation and our theoretical interpretation in Sec. VI. In Sec. VII we consider solitonic structures. By making comparisons between the geometrical soliton

structures and the spin-spin correlation functions, we show how they are closely related. We conclude and discuss in Sec. VIII.

As well as the work already mentioned, earlier work on the solitonic structure of the low-lying excitations include, a mean-field study of the Heisenberg-Peierls model,[21] and an exact diagonalization of a 12-site extended Hubbard-Peierls model.[22] The DMRG method was recently used by Yaron *et al.*[23] and Fano *et al.*[24] to solve the Pariser-Parr-Pople model for linear and cyclic polyenes, respectively.

II. PARISER-PARR-POPLE-PEIERLS MODEL

The Pariser-Parr-Pople-Peierls model is a realistic and accurate model of π-conjugated systems, which includes the key features of long-range electron-electron interactions and electron-lattice coupling. The Hamiltonian for an N site chain with open boundary conditions is defined as

$$\mathcal{H} = -2\sum_{l=1}^{N-1} t_l \hat{T}_l + \frac{1}{4\pi t_0 \lambda}\sum_{l=1}^{N-1}\Delta_l^2 + \Gamma\sum_{l=1}^{N-1}\Delta_l$$
$$+ U\sum_{i=1}^{N}\left(n_{i\uparrow}-\frac{1}{2}\right)\left(n_{i\downarrow}-\frac{1}{2}\right) + \sum_{\langle ij\rangle}V_{ij}(n_i-1)(n_j-1),$$

$$(1)$$

where $\langle ij\rangle$ indicates all pairs of sites, $t_l = [t_0 + (\Delta_l/2)]$, and

$$\hat{T}_l = \tfrac{1}{2}\sum_\sigma (c_{l+1\sigma}^\dagger c_{l\sigma} + \text{H.c.}) \qquad (2)$$

is the bond order operator of the lth bond. We use the Ohno function for the Coulomb interaction,

$$V_{ij} = U/\sqrt{1+\beta r_{ij}^2}, \qquad (3)$$

where $\beta = (U/14.397)^2$ and bond lengths are in Å. The dimensionless electron-phonon coupling constant λ is defined by

$$\lambda = \frac{2\alpha^2}{\pi K t_0}, \qquad (4)$$

where K is the elastic spring constant [estimated to be 46 eV Å^{-2} from Raman analysis of C-C stretching modes in *trans*-$(CH)_2$],[25] and α relates the actual distortion of the lth bond from equilibrium, δr_l, to Δ_l:

$$\delta r_l = \Delta_l/2\alpha. \qquad (5)$$

We take the undistorted chain to lie along the x axis, with the bonds oriented at 30° to this axis. Then, for fixed bond angles, the distorted chain coordinates are defined as

$$x_{ij} = x_{ij}^0 - \frac{\sqrt{3}}{4\alpha}\sum_{l=i}^{j-1}\Delta_l,$$

$$y_{ij} = y_{ij}^0 - \frac{1}{4\alpha}\sum_{l=i}^{j-1}\Delta_l(-1)^{l+1}, \qquad (6)$$

TABLE II. The density-density correlator as a function of distance.

j	$\langle (n_i-1)(n_{i+j}-1)\rangle$
1	-0.308
2	$+0.002$
3	-0.021
4	$+0.004$
5	-0.011

where

$$x^0_{ij}=\frac{\sqrt{3}}{2}a_0|j-i|$$

and

$$y^0_{ij}=0, \quad \text{if} \quad |j-i| \quad \text{even}$$

$$=\frac{a_0}{2}(-1)^{(i+1)} \quad \text{otherwise.} \tag{7}$$

a_0 ($=1.40$ Å) is the undistorted C-C bond length.

The force per bond, f_l, is

$$f_l=-\frac{\partial\langle\mathcal{H}\rangle}{\partial\,\delta r_l}. \tag{8}$$

Using the Hellmann-Feynman theorem, this can be rewritten as

$$f_l=-2\alpha\left(\frac{\Delta_l}{2\pi t_0\lambda}+\Gamma-\langle T_l\rangle\right)-\sum_{\langle ij\rangle}{}'\,\frac{U\beta}{2\alpha(1+\beta r_{ij}^2)^{3/2}}$$
$$\times\left(\frac{\sqrt{3}}{2}x_{ij}+\frac{(-1)^{(l+1)}}{2}y_{ij}\langle(n_i-1)(n_j-1)\rangle\right). \tag{9}$$

The prime over the sum indicates that the sum runs over all pairs of sites which span the lth bond. The contribution to the bond force from the Coulomb interaction is small compared to the kinetic-energy term: the value of the Coulomb force from the nearest-neighbor density-density correlator is approximately one-tenth of the kinetic term. Moreover, the density-density correlator alternates in sign and drops to less than one-tenth of the nearest-neighbor density-density correlator, so the sum over all bonds is also small. Table II shows the correlator for up to five nearest neighbors. We therefore only include the nearest-neighbor density-density correlator in the evaluation of the distorted geometry. (However, the full distorted geometry is used in the evaluation of the Coulomb interaction [Eq. (3)].)

Using this approximation, and setting $f_l=0$, the self-consistent equation for the equilibrium Δ_l is

$$\Delta_l=\left(\frac{2\pi\alpha t_0\lambda}{\alpha-C_l t_0\lambda}\right)(\langle T_l\rangle-\Gamma-C_l a_0), \tag{10}$$
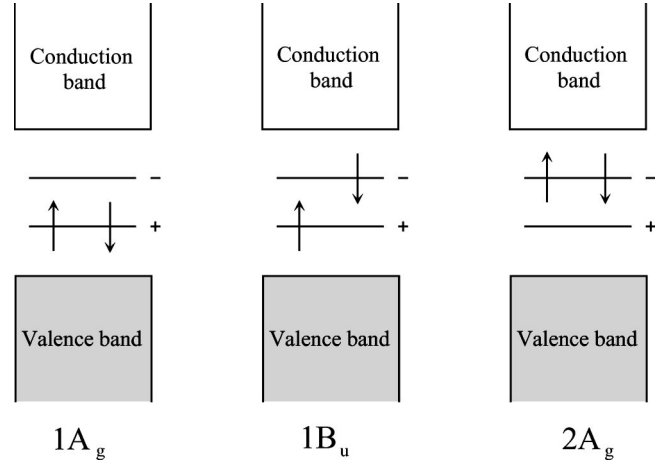
where

FIG. 1. Energy-level diagram for the key low-lying states in the noninteracting limit.

$$C_l=\frac{U\beta}{2\alpha[1+\beta(a_0+\delta r_l)^2]^{3/2}}\langle(n_l-1)(n_{l+1}-1)\rangle. \tag{11}$$

We observe that, since the nearest-neighbor density-density correlator is negative, the Coulomb interactions tend to increase the bond dimerization.

The calculations were performed for fixed chain lengths, which is enforced by setting

$$\Gamma=\frac{1}{N-1}\sum_{l=1}^{N-1}(\langle T_l\rangle-C_l a_0). \tag{12}$$

To complete our discussion of the model, we turn to its parametrization. There are three parameters in the model: t_0, U, and λ. An optimal parametrization for t_0 and U was found in Ref. 15 by fitting the Pariser-Parr-Pople model to the excited states of benzene. Assuming that this parametrization is transferable between all π-conjugated systems, we use them here, and set $t_0=2.539$ eV and $U=10.06$ eV. The remaining parameter λ is found by fitting the vertical energies of the $1\,^1B_u^-$ and $2\,^1A_g^+$ states, calculated from the Parsier-Parr-Pople-Peierls model, to the six-site linear polyene.[16] This gives $\lambda=0.115$. Finally, using $K=46$ eV Å^{-2} implies $\alpha=4.593$ eV Å^{-1}.

III. SOLUTION OF THE PEIERLS MODEL

As originally recognized by Pople and Walmsley,[26] the low-lying excitations of the dimerized even-N site chain correspond to the creation of two midgap states. These excitations are associated with localized geometrical structures, which lead to a reversal of the lattice dimerization, and were subsequently termed solitons. The defect states repel from each and are repelled from the ends of the chain. Thus, they reside at approximately $N/4$ and $3N/4$ along the chain [as may be seen in Fig. 5(b)]. Figure 1 shows a schematic energy diagram of the molecular orbitals and defect states, while Fig. 2 shows the energies of the $1\,^1B_u^-$ and $2\,^1A_g^+$ states as a function of inverse chain length. It is clear that the first excited even-parity state lies above the odd-parity state. How-
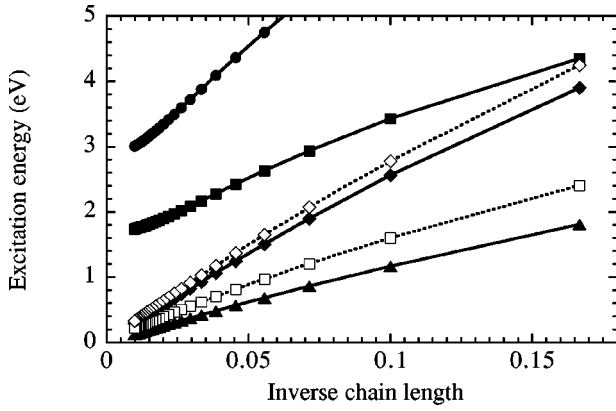
FIG. 2. Transition energies for the $1\,^1B_u^-$ (squares), $2\,^1A_g^+$ (diamonds), and $1\,^3B_u^+$ (triangles) states and the charge gap (circles) as functions of the inverse chain length for the $U=0$ Peierls model (dashed lines and open symbols) and the $\lambda=0$ Pariser-Parr-Pople model (solid lines and filled symbols). (In the Peierls model the $1\,^1B_u^-$ and $1\,^3B_u^+$ states are degenerate.)

ever, in the long chain, continuum limit, these states are degenerate, with energy $4\Delta_0/\pi=0.12$ eV, using $\lambda=0.115$, $t_0=2.539$ eV, and[27]

$$\Delta_0 = 8t_0 \exp\left[-\left(1 + \frac{1}{2\lambda}\right)\right]. \tag{13}$$

This gap is only a fraction of the experimentally measured gap of approximately 2.0 eV.[28] While a larger optical gap can be obtained by increasing λ and t_0, the energetic ordering of the low-lying states would still be incorrect. As we see in Sec. IV, it is electronic interactions which primarily open the optical gap, and reverse the energetic ordering of the states. Furthermore, electronic interactions significantly modify the soliton structures, as we show in Sec. VII.

The noninteracting limit enables us to make a comparison between the DMRG methods and the exact calculation. In Fig. 3 the energy difference between the exact results and DMRG calculations is shown for the $1\,^1B_u^-$ and $2\,^1A_g^+$ states. We see that for both states the accuracies of the infinite and finite lattice algorithm calculations are close, so that both methods can be used in the actual calculations. The accuracy is better for the $1\,^1B_u^-$ state, but even for the $2\,^1A_g^+$ the error is about 0.002 eV for the 50-site chain in the infinite lattice algorithm calculation. Other DMRG convergence tests, confirming the validity of the method, were presented in Ref. 16.

IV. SOLUTION OF THE PARISER-PARR-POPLE MODEL

The uniform chain in the limit of only on-site Coulomb interactions is described by the Hubbard model. At half-filling, the spin excitations are gapless in the infinite-chain limit, whereas the charge excitations are gapped. Even though the Pariser-Parr-Pople model contains long-range interactions, the spin excitations still appear to be gapless in the uniform chain, as shown in Fig. 2. The $2\,^1A_g^+$ state is also gapless, confirming the interpretation of it as a pair of bound magnons. The optical gap $[E(1\,^1B_u^-)]$ extrapolates to ap-
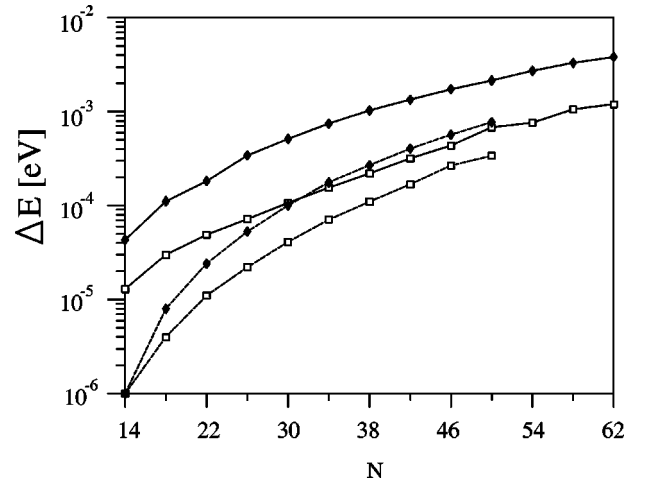

FIG. 3. The difference between the exact calculation of the $2\,^1A_g^+$ (diamonds) and $1\,^1B_u^-$ (squares) states in the noninteracting limit, and the results of DMRG calculations in infinite and finite algorithms. Solid lines correspond to the infinite lattice algorithm results, and dashed lines to the finite lattice algorithm.

proximately 1.6 eV, and is excitonic, lying approximately 1.0 eV below the charge gap for long chains. As discussed in Sec. I, the energies of the $2\,^1A_g^+$ and $1\,^1B_u^-$ states in polyacetylene thin films are believed to be at approximately 1.0 -1.8, and 2.0 eV, respectively. Approximately 0.3 eV should be deducted from the calculated $1\,^1B_u^-$ energy to account for solvation effects,[29] indicating that the undimerized Pariser-Parr-Pople model underestimates the optical gap by approximately 0.7 eV, and the $2\,^1A_g^+$ energy by up to 1.8 eV.

V. SOLUTION OF THE PARISER-PARR-POPLE-PEIERLS MODEL

Sections III and IV indicate that neither electron-lattice coupling nor electron-electron interactions alone are sufficient to explain the low-energy excitations of polyene oligomers. A pure electron-phonon model predicts degenerate $1\,^1B_u^-$ and $1\,^3B_u^+$ states with the $2\,^1A_g^+$ state lying above them, while a pure electron interaction model underestimates the optical gap, has gapless spin excitations and does not lead to a dimerized chain. We now turn to the DMRG solution of the Pariser-Parr-Pople-Peierls model. We note that an infinitesimally small electron-phonon coupling will open a gap in the spin excitation spectrum for all electronic interaction strengths.

We first calculate the ground-state energy and lattice geometry. The normalized staggered bond dimerization is defined as

$$\delta_l \equiv (-1)^l \frac{(t_l - \bar{t})}{\bar{t}}, \tag{14}$$

where $\bar{t}$ is the average value of t_l in the middle of the chain. $\delta=0.102$ in the center of the chain. Using $\alpha=4.593$ eV Å^{-1}, this implies that the bond-length alterna-
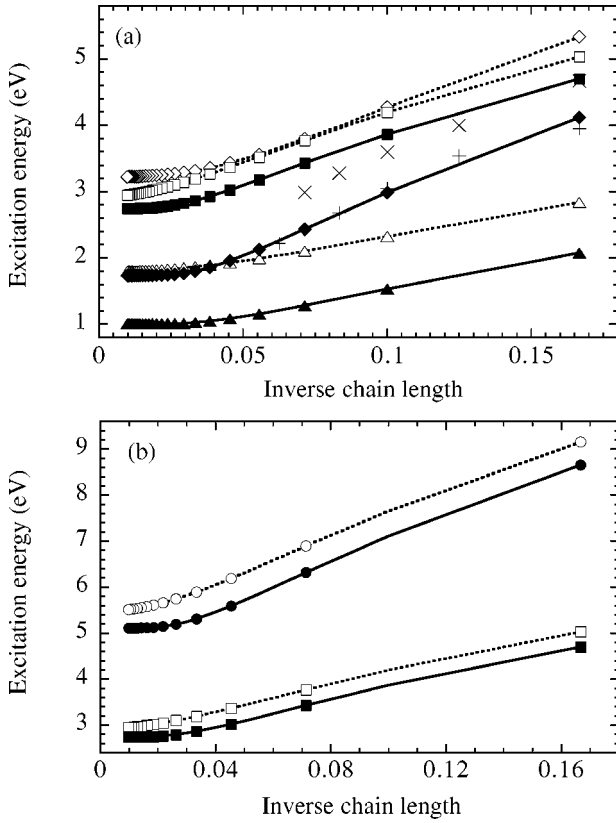
FIG. 4. (a) Transition energies for the $1\,^1B_u^-$ (squares), $2\,^1A_g^+$ (diamonds), and $1\,^3B_u^+$ (triangles) states as functions of the inverse chain length. Vertical and relaxed transitions are indicated by dashed and solid lines and open and solid symbols. Experimental results for the relaxed $1\,^1B_u^-$ ($\times$) and $2\,^1A_g^+$ ($+$) state energies for polyenes in hydrocarbon solution (Ref. 32). (b) Transition energies for the $1\,^1B_u^-$ state (squares) and charge gap (circles) as functions of the inverse chain length.

tion of the ground state in the middle of the chain is 0.056 Å, in close agreement with the experimental result of 0.052 Å.[30]

Using the ground-state geometry, the vertical energies (that is, the energies of these states with the ground-state geometry) (E^v) of the $1\,^3B_u^+$, $1\,^1B_u^-$, and $2\,^1A_g^+$ states are calculated. These, as well as the relaxed energies (E^{0-0}), are shown in Fig. 4(a) as functions of inverse chain length. The vertical energy of the $2\,^1A_g^+$ state lies approximately 0.3 eV above that of the $1\,^1B_u^-$ state in the long chain limit.[31] The relaxation energy of the $1\,^1B_u^-$ state is modest, being approximately 0.2 eV for 102 sites. By contrast, the relaxation energies of the $1\,^3B_u^+$ and $2\,^1A_g^+$ states are substantial, being approximately 0.8 and 1.5 eV, respectively, and converge rapidly with increasing chain length. The energy of the relaxed $2\,^1A_g^+$ state lies 1 eV below that of the $1\,^1B_u^-$ state. We see in Sec. VII that this strong relaxation is associated with a large distortion of the ground state structure.

In Fig. 4(b) we plot the charge gap,

$$E(N+1)+E(N-1)-2E(N), \qquad (15)$$

and the energy of the $1\,^1B_u^-$ state. In the long chain limit the charge gap represents the energy of an uncorrelated electron-hole pair, and therefore represents the band edge. The relaxation energy of the charge gap is roughly double that of the $1\,^1B_u^-$ state. This is to be expected, as the two charges form independent polarons, whereas the excitonic $1\,^1B_u^-$ state forms a single polaron, as discussed in Sec. VII. We see that the single chain binding energy is 2.4 eV. However, the unbound pair is strongly solvated (~ 1.5 eV), while the exciton is more weakly solvated (~ 0.3 eV).[29] This implies that the bulk binding energy of the $1\,^1B_u^-$ state is ~ 1 eV.

The experimental values of $E^{0-0}(1\,^1B_u^-)$ and $E^{0-0}(2\,^1A_g^+)$ for short polyenes are also shown.[32] The $2\,^1A_g^+$ values are in excellent agreement with our calculation. The $1\,^1B_u^-$ values are approximately 0.3 eV lower than our predictions, which is approximately the reduction expected by the solvation of the chains in solution.[29] Thus, for short polyene oligomers, the optimized parametrization of the Pariser-Parr-Pople-Peierls model gives remarkably good results.

Kohler analyzed the experimental results for $N=6-16$.[32] For the $2\,^1A_g^+$ state the empirical relation,

$$E^{0-0}(2\,^1A_g^+)=0.96+20.72/N, \qquad (16)$$

was derived. This relation appears to confirm the work of Ref. 11, whose authors found a $2\,^1A_g^+$ state at 1.1 eV in thin films. However, there is no particular reason why a linear extrapolation in $1/N$ is valid. Our calculation for the Pariser-Parr-Pople-Peierls model shows a significant flattening off of the $2\,^1A_g^+$ energy for chain lengths of roughly 30 or more sites. The calculated converged energy of 1.74 eV is in agreement with Ref. 13.

This rapid convergence of energy with chain length is in contrast to both the Pariser-Parr-Pople and Peierls models. In the Peierls model the excitation energies are gapped, but the deviation from $1/N$ behavior is only evident for long chains (~ 100 sites). In the Pariser-Parr-Pople model a deviation from $1/N$ behavior is only evident in the long chain limit for the $1\,^1B_u^-$ state and the charge gap. In the Pariser-Parr-Pople-Peierls model, however, states which form pronounced solitonic structures, such as the $2\,^1A_g^+$ and triplet states (as discussed in Sec. VII) self-trap once the chain length exceeds the size of their solitonic structures. It is possible that this self-trapping is a consequence of the adiabatic treatment of the lattice, and that a full treatment involving quantum phonons would change this prediction.

Our understanding of self-trapping—and its validity or otherwise—is complicated by the discussion of the $1\,^1B_u^-$ state energy. Again, an empirical relation,

$$E^{0-0}(1\,^1B_u^-)=2.01+15.60/N, \qquad (17)$$

was derived by Kohler, which is in good agreement with the thin film result. Our calculated value of 2.74 eV is too high, even when solvation effects (~ 0.3 eV) are deducted. Once again, the $1\,^1B_u^-$ state is self-trapped, and the possible relaxation by lattice fluctuations would lead to a better agreement.

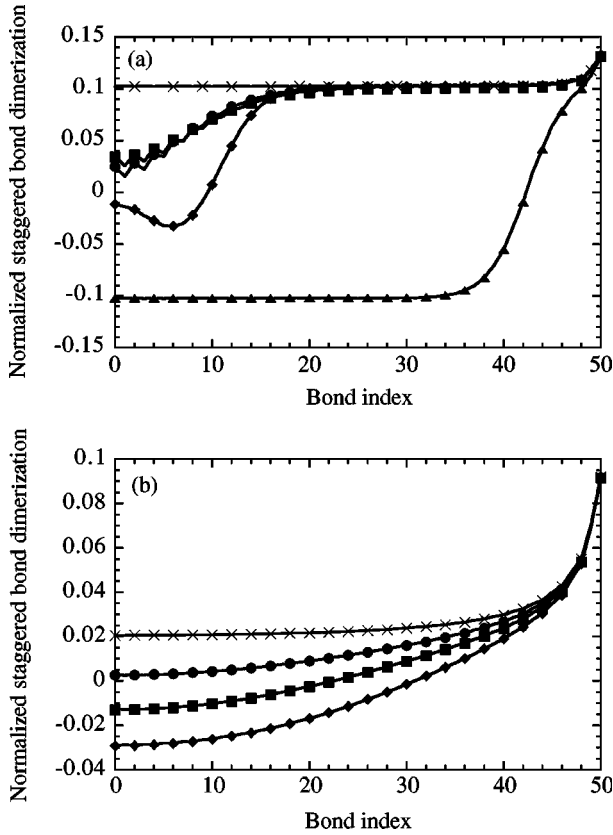However, since the phonon frequency of ~ 0.2 eV is so small compared to the electronic energy scales, any correc-

FIG. 5. (a) The geometries (normalized staggered bond distortion δ_l as a function of the bond index l from the center of the lattice) of various states of the Pariser-Parr-Pople-Peierls model: $1\,^1A_g^+$ (crosses), $1\,^1B_u^-$ (squares), $1\,^3B_u^+$ (triangles), $2\,^1A_g^+$ (diamonds), and polaron (circles), for a 102-site system. (b) The same as (a) for the $U=0$ Peierls model.

tions to the adiabatic limit are expected to be small, so we need to consider other possible reasons for the discrepancies in the long chain limit. One source is the possible renormalization of the Pariser-Parr-Pople-Peierls model parameters in the long chain limit; another is σ-electron screening.

VI. PHOTOINDUCED ABSORPTION

The photoinduced absorption spectrum of a system, obtained while it is being pumped at an energy above the optical gap, gives an insight into the excited states of that system.[12] Typically the system is pumped at 2.4 eV, and photoinduced absorption peaks are observed at 0.43 and 1.35 eV.

The higher-energy peak is believed to be intrinsic and has been ascribed to a bound soliton-anti-soliton pair.[33] A possible interpretation is that excitations to states above the vertical $1\,^1B_u^-$ state decay nonradiatively to the $2\,^1A_g^+$ state, which subsequently relaxes. The photoinduced absorption is then a vertical transition from the relaxed $2\,^1A_g^+$ state to a $^1B_u^-$ state. We find that the energy of the $1\,^1B_u^-$ state in the relaxed geometry of the $2\,^1A_g^+$ state lies 1.3 eV above the $2\,^1A_g^+$ state for 102 sites. However, the dipole moment is weak, being only $0.16\langle\mu\rangle_{1\,^1B_u^-}$ (where $\langle\mu\rangle_{1\,^1B_u^-}$ is the dipole
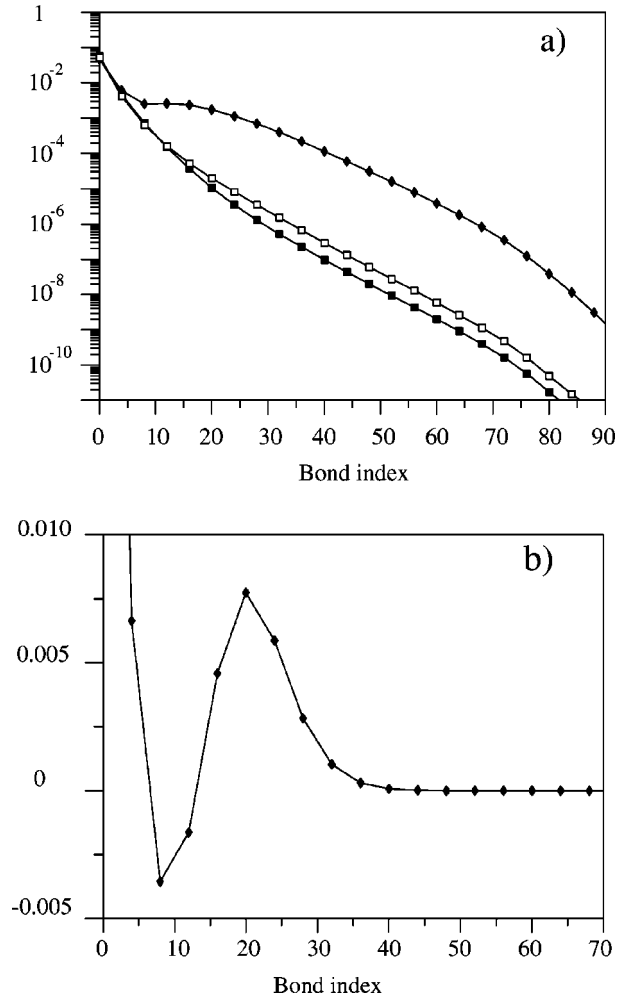

FIG. 6. Spin-spin correlation functions for $1\,^1A_g^+$ (solid squares), $2\,^1A_g^+$ (solid diamonds), and $1\,^1B_u^-$ (empty squares) states. (a) In the relaxed $1\,^1A_g^+$ geometry. (b) In the relaxed $2\,^1A_g^+$ geometry.

moment between the ground state and $1\,^1B_u^-$ state). A second possibility is that it is a triplet-triplet ($T\to T^*$) transition. We calculate this transition energy to be 2.8 eV, while the dipole moment is $0.96\langle\mu\rangle_{1\,^1B_u^-}$. Since the excited triplet (T^*) is a triplet exciton (as opposed to a spin-density wave excitation) at high energy, it is reasonably to assume that it will be strongly solvated, reducing this transition energy by as much as 1 eV. Thus a triplet to triplet transition is a possible explanation for this absorption.

We calculate the transition energy between the lowest polaron state and the first dipole connected excitation to be 0.45 eV at 102 sites, and the dipole moment is $0.88\langle\mu\rangle_{1\,^1B_u^-}$, suggesting that this is the origin of the lower peak.

VII. SOLITON STRUCTURES

In Fig. 5(a) we plot, as a function of bond index from the center of the chain, the normalized staggered bond dimerization, δ_l [Eq. (14)]. We note that the $1\,^3B_u^+$ and $2\,^1A_g^+$ states undergo considerable bond distortion, whereas the $1\,^1B_u^-$

state shows a weak polaronic distortion of the lattice, similar to the distortion associated with a doped charge. In Ref. 16 we showed that the $1\,^3B_u^+$ and $1\,^1B_u^-$ states fit a 2-soliton form,[7,34,35] whereas the $2\,^1A_g^+$ state fits a 4-soliton form. The bond distortions of the non-interacting limit (the Peierls model) are plotted in Fig. 5(b). A comparison between these plots illustrates the role played by the electronic interactions in modifying the noninteracting picture

(1) The dimerization in the ground state is enhanced by a fivefold factor, in qualitative agreement with Refs. 19 and 20.

(2) The $1\,^1B_u^-$ state evolves to an exciton-polaron, in agreement with Ref. 10.

(3) The $2\,^1A_g^+$ state, owing to its strong triplet-triplet contribution, evolves to a 4-soliton solution, in agreement with Ref. 6.

Further insight into the electronic structure of polyenes and its relation to their geometry can be obtained from the spin-spin correlation function, defined as

$$S_i = -\langle S_i^Z S_{N+1-i}^Z \rangle. \tag{18}$$

This function measures antiferromagnetic correlations between sites symmetrically situated with respect to the center of the chain. As the correlation function shows unimportant oscillations between even and odd site indices i, we use the symmetrized function

$$\tilde{S}_j = \tfrac{1}{2}(S_{(1/2)(N-j)} + S_{(1/2)(N-j)+1}), \tag{19}$$

$j = 0,4,8,\ldots,N-2$, which measures the correlations between pairs of doubly bonded sites, with j being the distance between them.

The spin-spin correlation functions, calculated in the ground state geometry, are shown in Fig. 6(a). They show a monotonic decay for the correlations in the $1\,^1A_g^+$ and $1\,^1B_u^-$ states, but in the $2\,^1A_g^+$ state there is a small minimum at $j = 8$ and a maximum at $j = 16$. This behavior of the spin-spin correlations in the $2\,^1A_g^+$ state becomes clearer when we calculate it in the relaxed geometry for this state. Here, the correlation function of the $2\,^1A_g^+$ state, shown in Fig. 6(b), has a strong minimum at $j = 8$, where it changes sign, and a maximum at $j = 20$. These features strongly confirm the triplet-triplet character of this state. By comparing Fig. 6(b) to the soliton structure shown in Fig. 5(a), we see that the unpaired spins correspond to the positions of the geometrical solitons.

VIII. DISCUSSION AND CONCLUSIONS

We began this investigation of the electronic and geometrical structure of linear polyenes by performing separate studies of the $U = 0$ Peierls model and the $\lambda = 0$ Pariser-Parr-Pople model. These studies show that these two limits predict quite different low-lying excitations. The Peierls model predicts midgap states associated with geometrical defects.

The dipole-forbidden $2\,^1A_g^+$ state lies above the degenerate singlet and triplet $1B_u$ states. In contrast, the Pariser-Parr-Pople model predicts gapless (or very small gapped) triplet and $2\,^1A_g^+$ states, with the $1\,^1B_u^-$ state lying above them.

When these two models are combined in the Pariser-Parr-Pople-Peierls model we see the effect of the interplay of electron-electron and electron-phonon interactions. The lowest-lying triplet ($1\,^3B_u^+$) is a soliton-antisoliton pair; the lowest-lying singlet ($2\,^1A_g^+$) is an even-parity pair of soliton-antisoliton pairs, owing to it being a bound pair of triplets; and the lowest optically allowed state ($1\,^1B_u^-$) is an exciton-polaron. The soliton positions in the $2\,^1A_g^+$ state is confirmed by the spin-spin correlation function. Electron-electron interactions play the dominant role in opening the optical gap and dimerizing the lattice.

We find that the relaxation energies of the $1\,^3B_u^+$ and $2\,^1A_g^+$ states are substantial, whereas the energy of the $1\,^1B_u^-$ state is modest. The vertical energy of the $2\,^1A_g^+$ state lies above that of the $1\,^1B_u^-$ state, but the relaxed $2\,^1A_g^+$ state lies ~ 1.0 eV below that of the $1\,^1B_u^-$ state. The role of electron-electron interactions are crucial and subtle in determining these relative positions. A larger electron-electron interaction leads to a more dimerized ground state, and this tends to raise the vertical energy of the $2\,^1A_g^+$ state relative to that of the $1\,^1B_u^-$ state. However, a larger electron-electron interaction also leads to a larger relaxation of the $2\,^1A_g^+$ state energy compared to that of the $1\,^1B_u^-$ state, leading to a reversal of their energies.

For short polyenes we find good agreement with experimental values. However, in the long chain limit the results (at least for the $1\,^1B_u^-$ state) become more qualitative. The experimental uncertainty in the position of the $2\,^1A_g^+$ state means that we cannot be sure of the validity of our prediction. However, if we assume that ~ 1.0 eV is the correct relaxed energy of the $2\,^1A_g^+$ state, then our predictions are between 0.5 and 1.0 eV too high. In Sec. V we discussed some of the possible origins of these discrepancies. They include, the neglect of lattice fluctuations in the adiabatic treatment of the lattice, the possible renormalization of the π-model parameters in the long chain limit, and the neglect of the σ-bond screening. We would expect that as a molecule gets larger the π orbitals will become more extended, as they mix with other orbitals. This will reduce U and α (and hence λ), and increase t_0, thus reducing the excitation energies. Work is currently in progress to study these affects.

*Email address: W.Barford@sheffield.ac.uk

†Current address: The School of Chemistry, University of Bristol, Bristol, U.K. On leave from Institute of Inorganic Chemistry, 630090 Novosibirsk, Russia.

[1] As defined by the energy to add a particle and a hole to a half-filled system.

[2] B. S. Hudson and B. E. Kohler, Chem. Phys. Lett. **14**, 299 (1972).

[3] K. Schulten and M. Karpus, Chem. Phys. Lett. **14**, 305 (1972).

[4] P. Tavan and K. Schulten, Phys. Rev. B **36**, 4337 (1987).

[5] R. R. Birge, K. Schulten, and M. Karplus, Chem. Phys. Lett. **31**, 451 (1975); R. McDiarmid, J. Chem. Phys. **79**, 1565 (1983); B. Hudson and B. Kohler, Synth. Met. **9**, 241 (1984).

[6] G. W. Hayden and E. J. Mele, Phys. Rev. B **34**, 5484 (1986).

[7] W. P. Su, Phys. Rev. Lett. **74**, 1167 (1995).

[8] G.-Z. Wen and W.-P. Su, *Relaxations of Excited States and Photo-induced Structural Phase Transitions* (Springer-Verlag, Berlin, 1997), p. 121; Synth. Met. **78**, 195 (1996).

[9] A. A. Ovchinnikov, I. I. Ukrainskii, and G. V. Kventsel, Usp. Fiz. Nauk. **108**, 81 (1973) [Sov. Phys. Usp. **15**, 575 (1973)].

[10] M. Grabowski, D. Hone, and J. R. Schrieffer, Phys. Rev. B **31**, 7850 (1985).

[11] C. Halvorson and A. J. Heeger, Chem. Phys. Lett. **216**, 488 (1993).

[12] *Relaxation in Polymers*, edited by T. Kobayashi (World Scientific, Singapore, 1993), p. 174.

[13] W.-S. Fann, S. Benson, J. M. J. Madey, S. Etemad, G. L. Baker, and F. Kajzar, Phys. Rev. Lett. **62**, 1492 (1989).

[14] D. Baeriswyl, D. K. Campbell, and S. Mazumdar, in *Conjugated Conducting Polymers*, edited by H. Kiess (Springer-Verlag, Berlin, 1992).

[15] R. J. Bursill, C. Castleton, and W. Barford, Chem. Phys. Lett. **294**, 305 (1998).

[16] R. J. Bursill and W. Barford, Phys. Rev. Lett. **82**, 1514 (1999).

[17] S. R. White, Phys. Rev. Lett. **69**, 2863 (1992); Phys. Rev. B **48**, 10 345 (1993).

[18] *Density Matrix Renormalization*, edited by I. Peschel, X. Wang, M. Kaulke, and K. Hallberg (Springer, Berlin, 1999).

[19] P. Horsch, Phys. Rev. B **24**, 7351 (1981).

[20] G. Konig and G. Stollhoff, Phys. Rev. Lett. **65**, 1239 (1990).

[21] J. Takimoto and M. Sasai, Phys. Rev. B **39**, 8511 (1989).

[22] J. T. Gammel and D. K. Campbell, Synth. Met. **55**, 4638 (1993).

[23] D. Yaron, E. E. Moore, Z. Shuai, and J. J. Bredas, J. Chem. Phys. **108**, 7451 (1998).

[24] G. Fano, F. Ortolani, and L. Ziosi, J. Chem. Phys. **108**, 9246 (1998).

[25] E. Ehrenfreund, Z. Vardeny, O. Barfman, and B. Horovitz, Phys. Rev. B **36**, 1535 (1987).

[26] J. A. Pople and S. H. Walmsley, Mol. Phys. **5**, 15 (1962).

[27] A. J. Heeger, S. Kivelson, J. R. Schrieffer, and W-P. Su, Rev. Mod. Phys. **60**, 781 (1988).

[28] However, the exact $1\,{}^1B_u^-$ transition energy obtained from Eq. (1) at 102 sites is 0.23 eV, while the $2\,{}^1A_g^+$ state is at 0.33 eV.

[29] E. Moore, B. Gherman, and D. Yaron, J. Chem. Phys. **106**, 4216 (1997).

[30] H. Kahlert, O. Leitner, and G. Leising, Synth. Met. **17**, 467 (1987).

[31] Experimentally, this implies that the vertical energy of the $2\,{}^1A_g^+$ state lies about 0.6 eV above the $1\,{}^1B_u^-$ state, because of the greater solvation energy of the latter state.

[32] B. E. Kohler, J. Chem. Phys. **88**, 2788 (1988).

[33] J. Orenstein and G. L. Baker, Phys. Rev. Lett. **49**, 1043 (1982).

[34] D. K. Campbell and A. R. Bishop, Nucl. Phys. B **200**, 297 (1982).

[35] M. A. Garcia-Bach, R. Valenti, S. A. Alexander, and D. J. Klein, Croat. Chem. Acta **64**, 415 (1991).